Tuning the Properties of Hydrogel Microspheres by Adding Chemical Crosslinking Functionality to Sodium Alginate

Redouan Mahou,[‡,‡] Françoise Borcard,[‡,‡] Virginia Crivelli,[‡,‡] Elisa Montanari,[#] Solène Passemard,[‡] François Noverraz,[‡] Sandrine Gerber-Lemaire,[*,‡] Léo Bühler,[#] and Christine Wandrey[*,‡]

[‡]Institut d'Ingénierie Biologique et Institut des Sciences et Ingénierie Chimiques, Ecole Polytechnique Fédérale de Lausanne, EPFL-SV-IBI-LMRP, station 15, CH-1015 Lausanne, Switzerland

[#]University Hospital of Geneva, Surgical Research Unit, CMU-1, rue Gabrielle-Perret-Gentil, CH-1211 Geneva, Switzerland

Supporting Information

ABSTRACT: Two novel types of hydrogel microspheres (MS) are presented. First, one-component microspheres (1-comMS) were produced from sodium alginate (Na-alg) equipped with thiol-functionalized hydroxyl groups. The functionalization pathway included the conversion of Na-alg into tetrabutylammonium alginate, insertion of new carboxyl groups, grafting of α-amine-ω-thiol poly(ethylene glycol), and restoration of the sodium salt. This modification conserves all original carboxyl groups of Na-alg and allows for covalent disulfide bond formation in addition to ionic crosslinking. Second, two-component microspheres (2-comMS) were obtained from a mixture of Na-alg and Na-alg functionalized with cysteamine. This functionalization was achieved by grafting cystamine dihydrochloride on some carboxyl groups followed by the reduction to cysteamine. Using the one-step MS formation process developed for both MS types, very fast ionic gelation with calcium ions conserves the spherical shape of the polymer solution droplets upon extrusion into the gelation bath, while simultaneously occurring slow covalent crosslinking reinforces the hydrogels. The physical properties of both MS types are adjustable by varying the polymer concentration, the degree of grafting, and the mixing ratio. In vitro cell microencapsulation studies confirmed the cytocompatibility of 1-comMS and 2-comMS.

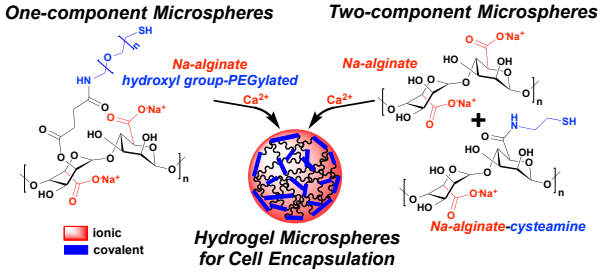

INTRODUCTION

The water-soluble biopolymer sodium alginate (Na-alg) spontaneously forms hydrogels under mild conditions of pH and temperature upon replacing the sodium ions by divalent cations.[1-6] In particular, the hydrogel calcium alginate (Ca-alg) is considered suitable for a variety of pharmaceutical, biological and medical applications including cell immobilization.[7,8] A special application is the entrapment of cells in micro-sized 3D hydrogels. The small dimension of such microspheres (MS) provides an optimal surface/volume ratio and is favorable for the mass transfer between cells and their environment, presupposed that the hydrogel is sufficiently stable and has the desired network density. Immobilization of cells in hydrogel MS is the prerequisite for the success of several cell therapies that are currently under development or in clinical trials. Some examples that highlight the variety of potential applications are external organ support,[9] treatments relying on cell allo- or xenotransplantation,[10,11] and prosthetic gene networks.[12,13] However, for alginate-based MS prepared by only ionic crosslinking with divalent cations, insufficient mechanical properties, stability and permselectivity have been argued.[5,14-17] Moreover, due to the lack of optimal materials, which meet the general requirements for cell microencapsulation and which in addition can be adapted to the needs of specific cell types and applications, the development of innovative cell therapies is slowly progressing.

To address these issues, different strategies have focused on either the improvement of Ca-alg MS or the replacement of Ca-alg by other materials. Despite some progress, coating Ca-alg MS with polycations such as poly(L-lysine),[18-23] poly(L-ornithine)[24,25] or poly(methylene guanidine)[26-28] or employing other polymers[10,29-36] was frequently accompanied by reduced biocompatibility, and also more complicated multi-step MS formation processes were required.[37-40] In another way, promising approaches include the development of alginate derivatives with enhanced performance and the combination of Na-alg with poly(ethylene glycol) (PEG).[41-51] In accordance with this concept, we have recently developed two types of Na-alg-based MS produced by a one-step process, and we have shown their suitability for cell microencapsulation.[11,52-54] The first was a one-component MS (1-comMS) formed from a Na-alg derivative with heterobifunctional PEG grafted on the carboxyl groups.[52] The other was a two-component MS (2-comMS) composed of an interpenetrating polymer network of Ca-alg and covalently crosslinked vinyl sulfone-terminated multi-arm poly(ethylene glycol).[11, 53,54]

The overall objective of the present study was to further extend the material basis for cell microencapsulation, i.e., to synthesize Na-alg derivatives, which yield in one-step processes MS with favorable and tunable properties. First, we modified hydroxyl groups of Na-alg to allow the grafting of α-amine-ω-thiol-poly(ethylene glycol),

so maintaining all carboxyl groups for ionic crosslinking. Second, another reagent than PEG derivatives, cyteamine, was used for the Na-alg functionalization. The resulting Na-alg derivatives and hydrogels were characterized in terms of chemical composition, stability, permeability and mechanical resistance. Finally, the cytocompatibility of 1-comMS and 2-comMS, produced either from PEG-grafted Na-alg or from cysteamine grafted Na-alg mixed with Na-alg, was evaluated by microencapsulation of primary human foreskin fibroblasts (EDX cells).

EXPERIMENTAL SECTION

Materials. Na-alg Kelton HV (lot no. 61650A, $[\eta]$ = 813 mL g^{-1} in 0.1 M NaCl, T = 25 °C, G/M = 0.6) and Na-alg Kelton LV (lot no. 46198A, $[\eta]$ = 475 mL g^{-1} in 0.1 M NaCl, G/M = 0.69) were obtained from Kelco (San Diego, USA, CA). Na-alg PRONOVA UP LVM was from FMC BioPolymer (Novamatrix, Drammen, Norway, batch no FP-506-01, $[\eta]$ = 405 mL g^{-1} in 0.1 M NaCl).[55,56] α-amine-ω-thiol-poly(ethylene glycol) (NH_2-PEG-SH, 2000 g mol^{-1}) was purchased from JenKem (JenKem Technology USA, Allen, TX, USA). Tetrabutylammonium hydroxide (TBAOH), N-(3-dimethylaminopropyl)-N′-ethylcarbodiimide hydrochloride (EDC), 2-(N-morpholino) ethanesulfonic acid (MES), sodium cyanoborohydride ($NaCNBH_3$), tris(2-carboxylethyl)phosphine hydrochloride (TCEP), cystamine dihydrochloride, 3-(N-morpholino)propanesulfonic acid (MOPS), calcium chloride dihydrate ($CaCl_2{\cdot}2H_2O$), fluorescein isothiocyanate-dextran (FITC-dextran, 40, 70 and 150 kg mol^{-1}), as well as all other common reagents and solvents were purchased from Sigma (Sigma-Aldrich, Switzerland). All reagents were analytical grade and were used without further purification. Dialysis bags (Visking type 36/32, cellulose, MWCO 14 kg mol^{-1}) were obtained from Carl Roth (Karlsruhe, Germany).

Synthesis Pathway of Na-alg-PEG (Scheme 1). To convert Na-alg (1) into alginic acid, Kelton HV (4 g) was added to a mixture of aqueous HCl (60 mL, 0.6 N) and ethanol (60 mL), and the solution was stirred overnight at 4 °C. The resulting solid was separated by vacuum filtration, washed with ethanol and acetone, and dried overnight under vacuum at 40 °C. Dried alginic acid was dispersed in water (200 mL), and TBAOH (40% in water) was added dropwise until the polymer was fully dissolved. The pH was adjusted between 7 and 10, and the solution was dialyzed and finally freeze-dried to afford TBA-alg (2) as a white solid. Under nitrogen atmosphere, DMSO (10 mL) was added to TBA-alg (2) (150 mg, 1 equiv.) in a flask equipped with condenser, and the suspension was stirred at RT until good dispersion. Upon addition of molecular sieves, the temperature was raised to 40 °C. The amounts reported subsequently refer to reaction conditions no. 13 presented in the Supporting Information (SI) (SI 1, Table S1). Succinic anhydride (0.7 g, 7.1 mmol, 2 equiv.) and pyridine (0.05 mL, 6.1 mmol, 1.7 equiv.) were added, and the reaction mixture was stirred for 1 h at 40 °C. The polymer was precipitated by addition of ethyl acetate, filtered, and dried under vacuum. The crude product was dissolved in water, dialyzed (3 days), and freeze-dried to afford compound (5) as a white solid. Compound (5) (100 mg, 1 equiv.) and MES (150 mg) were dissolved in 10 mL of water and stirred at RT until good dispersion. NH_2-PEG-SH (77.4 mg, 0.2 equiv.) was added, followed by EDC (81.6 mg, 2.2 equiv.). The reaction mixture was stirred for 2 h at RT. TCEP (0.5 mL, 1 M) and MES (5 mL, 0.12 mg mL^{-1}) were added to the polymer solution inside the dialysis tube prior to the dialysis and then at each water exchange (twice daily for 2 days). At day 2, the pH was adjusted between 7 and 8 and the dialysis continued for one day in the presence of TCEP (0.5 mL, 1 M). After adjustment of the pH and two filtrations (70 μm and 0.22 μm), the product was freeze-dried to yield Na-alg-PEG (4) as a white solid.

Synthesis Pathway of Na-alg-cys (Scheme 2). Na-alg Kelton HV (1 g, 5 mmol) and MES (1.2 g, 5.5 mmol) were dissolved in 100 mL of distilled water and shaken at 4 °C until complete dissolution. Cystamine dihydrochloride (2.25 g, 10 mmol) was added. After stirring for 10 min at RT, EDC (900, 700, or 500 mg) was added and stirring was continued for 2 h at RT. The mixture was dialyzed against distilled water for 24 h and freeze-dried. The resulting solid was re-dissolved in a solution containing 100 mM TCEP in 10 mM MOPS (1 g polymer in 50 mL solution). Purification was achieved by 24 h dialysis against distilled water with four times water replacement. The purified solution was filtered (0.22 μm) and lyophilized yielding Na-alg-cys-500, Na-alg-cys-700, or Na-alg-cys-900 (5) as white solids.

Analytical Techniques. ^{1}H-NMR spectra were recorded on a Bruker-ARX-400 spectrometer (400 MHz); the chemical shift was referred to the solvent peak (δ = 4.79 for deuterium oxide). ^{13}C-NMR spectra were recorded on a Bruker-DRX-600 spectrometer (600 MHz, cryo). FTIR spectra were recorded on a Perkin Elmer spectrometer (Spectrum One) equipped with Spectrum software (version 5.3, Perkin Elmer). A rolling-ball viscometer (Lovis 2000 ME, Anton Paar, Graz, Austria) was used to measure both the solution viscosity and intrinsic viscosity. The osmolality was controlled by a Fiske micro-osmometer (model 210, Fiske Associates, Norwood, USA). Ellman's assay served to estimate thiol concentrations using the procedure described in the SI (SI 2).[57,58]

Formation of 1-comMS and 2-comMS. Fresh polymer solutions containing Na-alg-PEG or a mixture of Na-alg and Na-alg-cys-900 were prepared as detailed in the SI (SI 3, Table S2; SI 4 Tables S3 and S4). Unless noted otherwise, MOPS (10 mM, pH=7.4) was used as medium. 1-comMS and 2-comMS were produced employing a coaxial air-flow droplet generator (Encapsulator B-395 Pro, Büchi Labortechnik AG, Flawil, Switzerland). The polymer solution, with or without cells, was extruded into the tenfold volume of the gelation bath containing $CaCl_2 \cdot 2H_2O$ (100 mM) in MOPS. The MS were collected by filtration, washed twice with $CaCl_2$ stock solution, and finally stored in this solution at 4 °C, or in cell culture medium in case of cell microencapsulation.

Physical Characterization of 1-comMS and 2-comMS. Simultaneous formation of ionic and covalent crosslinks was qualitatively analyzed by treatment with sodium citrate (100 mM) or TCEP (0.5 M). The size (swelling or shrinking) of the MS in different media, at RT and 37 °C, was assessed on 30 MS randomly taken at defined time points. The average diameter was measured on an Olympus AX70 microscope equipped with an Olympus DP70 color digital camera. The water uptake was determined gravimetrically comparing the mass of the swollen and freeze-dried MS as reported previously.[53] The mechanical resistance to 90% compression of the initial MS diameter was analyzed using a texture analyzer (TA-XT2i, software Texture Exponent 32, Stable Micro Systems, Godalming, UK) equipped with a force transducer (1 mN resolution). A single MS was placed below the probe, for which a constant speed was set as 0.5 mm s^{-1}. Thirty MS of each batch were included in the analysis. The permeability of the MS was studied by measuring the ingress diffusion of FITC-dextran standards (40, 70, 150 kg

mol^{-1}). Prior to the measurement, the MS were equilibrated in the gelation bath. 700 mg of MS, collected by filtration and gently dried on paper, were incubated in 1 mL of FITC-dextran solution (1 mg mL^{-1} in 100 mM $CaCl_2$ solution). 40 µL of the supernatant were withdrawn after 1 min (t = 0) and at defined time intervals, and diluted in 600 µL of the gelation bath. Fluorescence spectroscopy (Multiplate Reader Safire- II Tecan, Maennedorf, Switzerland) was used to monitor the FITC-dextran concentration.

Microencapsulation of EDX Cells. Primary human foreskin fibroblasts (herein designated as EDX cells, provided by DFB Bioscience) were cultured and prepared for the microencapsulation as described previously.[54] Microencapsulation was performed using a 3.5 wt % solution of Na-alg-PEG-13 and the Na-alg-cys-900/Na-alg solution described in the SI (Table S4). Encapsulated EDX cells were cultured in Iscove's modified Dulbecco's Medium (IMDM) (Cambrex, Verviers, Belgium) supplemented with 10% fetal calf serum (Invitrogen, Basel, Switzerland), 100 IU mL^{-1} penicillin, 100 mg mL^{-1} streptomycin (Gibco-Invitrogen), dithiothreitol (Sigma, St-Louis, USA) and 10 ng mL^{-1} Platelet Derived Growth Factor BB (PDGF-BB, Peprotech EC Ltd, London, UK). The medium was changed every 3 days until one month of culture.

To assess viability and mortality, encapsulated cells were stained with fluorescein diacetate (FDA) and propidium iodide (PI) for 2 min and images were taken by fluorescence microscopy.[54] MS are permeable to FDA and PI, so that these stains can be used for assessment of encapsulated cells. The data was quantified using ImageJ software (http://rsbweb.nih.gov/ij)

Statistics. Unless otherwise noted, the results were expressed as the mean ± standard deviation (SD).

RESULTS AND DISCUSSION

Functionalization of Na-alg with PEG. Two principal synthesis pathways were followed for the functionalization of Na-alg hydroxyl groups with heterobifunctional PEG. Both routes functionalization of Na-alg by oxidation of the hydroxyl groups[59] and functionalization of Na-alg by esterification derivatization allowed for successful chemical modification of Na-alg. Nevertheless, only the functionalization according to Scheme 1 yielded a product, which was usable to form stable MS. The synthesis steps of the other pathway are presented in the SI (Scheme S1).[60,61]

The synthesis presented in Scheme 1 started with the conversion of Na-alg (**1**) into TBA-alg (**2**) with the intention to increase the solubility in organic solvents, thereby allowing the use of several organic media for a wider variety of functionalization reactions.[62,63] Spectroscopic analyses confirmed the TBA-alg structure (SI 5, Figure S1). In particular, the ^{1}H-NMR spectrum of compound (**2**) revealed peaks at 3.12, 1.57, 1.28, and 0.86 ppm corresponding to CH_2 and CH_3 moieties of the butyl residues. Insertion of new carboxylate groups was achieved via the reaction of TBA-alg with succinic anhydride in the presence of pyridine in DMSO.[62-64] This approach allows preferential functionalization of the mannuronic acid residues of the alginate backbone, as these are more soluble in DMSO, thereby keeping the less sterically hindered guluronic acid residues available for ionic crosslinking. The derivatization occurred favorably on the hydroxyl group in C3 position of the mannuronic residue and on the hydroxyl group in C2 position of the guluronic residue because the other hydroxyl groups are involved in a 1,3 diaxial interaction.[62,63] NH_2-PEG-SH was conjugated to the intermediate (**3**) through a coupling reaction to afford compound (**4**) which displays terminal thiol moieties for covalent crosslinking. The expected chemical structures were confirmed by spectroscopy (SI 5, Figures S2 and S3). The ^{1}H-NMR spectrum of compound (**4**) displayed peaks at 3.57 and 1.03 ppm corresponding to PEG CH_2 groups and SH moieties, respectively. In the ^{13}C-NMR spectra, peaks at 176.3, 174.0 and 172.7 ppm give evidence for the presence of ester, carboxylate and amide C=O moieties.

Scheme 1. Synthesis of Na-alg-PEG (4): Functionalization of Na-alg by esterification derivatization.

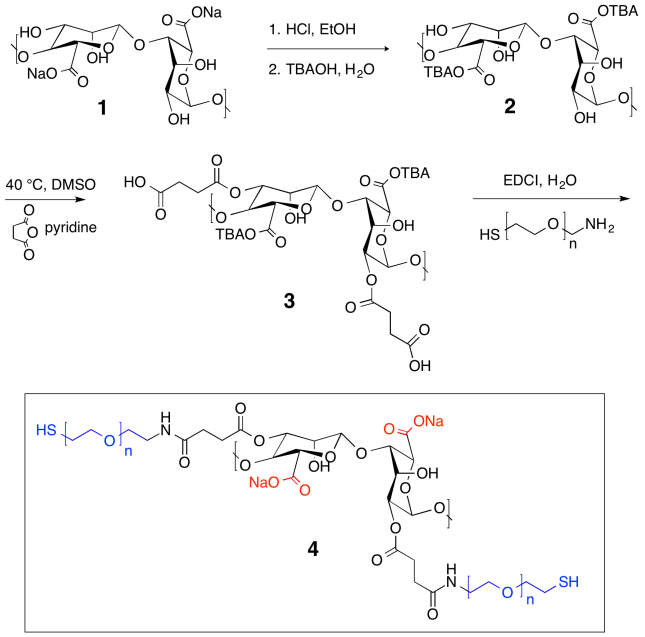

Screening different reaction and purification conditions (SI 1, Table S1) served to identify optimal protocols to yield Na-alg-PEG able to form stable, mechanically resistant 1-comMS. To identify the optimal conditions for the esterification reaction, different amounts of succinic anhydride/pyridine reagents were added and the reaction time was set at 1 or 2 h. As already demonstrated by Pawar et al.[62] for the acetylation of the alginate backbone, the reaction time strongly affects the molar mass reduction of TBA-alg, indicated by the viscosity of the solutions (Table 1). Either a low amount of succinic anhydride/pyridine (0.5 equiv./0.43 equiv.) for 2 h, or 2 equiv./1.7 equiv. of succinic anhydride/pyridine for 1 h, yielded intermediate products (**3**) allowing the formation of stable 1-comMS upon coupling of NH_2-PEG-SH.

The conjugation of the PEG derivative to intermediate (**3**) required a low amount of NH_2-PEG-SH (0.2 equiv.) in combination with EDC (2.2 equiv.) as coupling reagent to yield the desired grafted Na-alg-PEG. Coupling reagents allowing the reaction to occur in water were preferred. A mixture of NHS/EDC was also used, and resulted in completion of the reaction after 30 min (entries 1-4 in Table S1).[65] However, to hydrolyze the residual NHS-activated carboxylic acid groups at the end of the reaction, NaOH was required which caused substantial degradation of the alginate backbone chain. As result of the optimization, only EDC was selected as coupling reagent and the reaction time was fixed to 2 h.[65,66] Unreacted activated carboxylic acid was hydrolyzed during the

dialysis step by adding a solution of MES, slightly acidic, accelerating the hydrolysis reaction.[67]

Table 1. Optimized Conditions to Produce Na-alg-PEG

reagent/parameter	product	
	Na-alg-PEG-11	Na-alg-PEG-13
esterification		
succinic anhydride (equiv.)	0.5	2.0
pyridine (equiv.)	0.43	1.7
time (h)	2	1
temperature (°C)	40	40
viscosity[a] (mPa s)	384	541
grafting		
NH_2-PEG-SH (equiv.)	0.2	0.2
EDC (equiv.)	2.2	2.2
time (h)	2	2
temperature (°C)	RT	RT
degree of grafting[b] (%)	5	5

[a] viscosity of the solution containing 2.5 wt % intermediate (**5**). [b]by ^{1}H-NMR

The addition of an optimized amount of TCEP, as specified in the experimental section, prevented disulfide bond formation during the purification by dialysis. The optimization of this amount ensured that no excess of TCEP was left in the final product. MES served as buffer to facilitate the hydrolysis of the activated carboxylic acid. Neutralization was performed at day 2 of the dialysis. EDC liberates hydrochloric acid during the coupling reaction, and consequently TBA-alg was partially converted into alginic acid. Adjusting the pH between 7 and 8 (NaOH) led to regeneration of the sodium salt. Two reaction conditions out of 15 (SI 1, Table S1, entries 11 and 13) were finally identified to yield PEG-functionalized Na-alg able to form the expected 1-comMS upon extrusion of the polymer solution into the gelation bath containing only $CaCl_2$ as crosslinker.

Functionalization of Na-alg with Cysteamine. Na-alg-cys (**5**) was prepared as shown in Scheme 2, with Kelton HV as the starting Na-alg.

Scheme 2. Synthesis of Na-alg-cys (5): Functionalization of Na-alg with cystamine dihydrochloride via amide bonding followed by disulfide bond reduction.

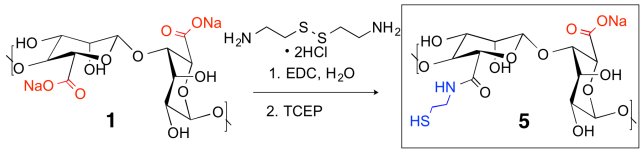

The efficiency of the graft reaction, that takes place at the carboxyl groups, was confirmed by ^{1}H-NMR and ^{13}C-NMR (SI 5, Figure S4). The ^{1}H-NMR spectrum showed two peaks (2.62 and 3.1 ppm) corresponding to cysteamine. Grafting evidence was provided by ^{13}C-NMR. A single signal of carboxylate groups was detected for the native Na-alg while for Na-alg-cys a new peak appeared at 160.6 ppm downfield by approx. 15 ppm in comparison with the corresponding alginate carboxyl. This new peak is attributed to the carbonyl of the amide group. Together, these results suggest that the cysteamine moieties that remained after dialysis are grafted onto the Na-alg backbone. The degree of grafting, which refers to the percent of modified carboxylate groups on Na-alg, was quantified by both ^{1}H-NMR and Ellman's assay (SI 2).[57] Adding different amounts of EDC to the reaction mixture (500, 700, 900 mg) yields products with different degrees of grafting (Figure 1). The ^{1}H-NMR analysis always yielded about 5% higher values for the degree of grafting than Ellman's assay. This deviation exceeds the error of the individual methods, but seems to be a systematic error. To avoid discrepancies related to the degree of grafting, exclusively Na-alg-cys-900 was subsequently used for all experiments in this study.

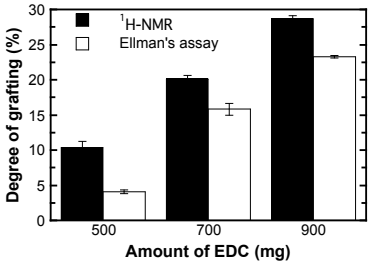

Figure 1. Degree of grafting as a function of the EDC amount added to the reaction, comparison of ^{1}H-NMR and Ellman's assay.[57] The error bars refer to the SD of n = 3 independent reactions.

The functionalization was accompanied by chain degradation. Compared to the intrinsic viscosity of the starting Na-alg Kelton HV (813 mL g^{-1} in 0.1 M NaCl, T = 25°C), the intrinsic viscosity of the graft product Na-alg-cys-900 (216 mL g^{-1}) was significantly lower.

Hydrogel Formation by Grafted Disulfide Bonds. Spontaneous hydrogel formation was observed upon exposure of Na-alg-PEG or Na-alg-cys solutions to air. The degree of grafting, the polymer concentration and the temperature govern the gelation rate. The photographs of Figure 2 confirm the disulfide bond formation for Na-alg-cys.[68]

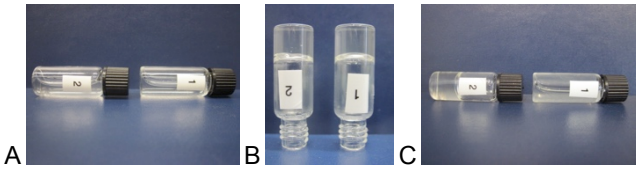

Figure 2. Confirmation of disulfide bond formation. (A) Clear solutions of Na-alg-cys-900 (2 wt % in MOPS); (B) chemical hydrogel via spontaneous disulfide bond formation at RT; (C) dissolution of the hydrogel upon adding the reducing agent TCEP to vial 1.

In this figure, the complete dissolution of Na-alg-cys-900 (20 mg) in MOPS (1 mL) was achieved in vial 1 and 2 after a few minutes shaking (Figure 2A). Spontaneous hydrogel formation took place within 36 h storage at RT without adding any crosslinker to the solutions (Figure 2B). Adding TCEP (200 µL, 0.5 M in water) to vial 1 and only 200 µL pure water to vial 2 confirmed that the gel formation is driven by disulfide bond formation. As visible in Figure 2C, the hydrogel in vial 1 was completely dissolved due to the reduction of disulfide bonds by TCEP, while the hydrogel in vial 2

did only absorb some water, which led to slight increase of the hydrogel volume (swelling). A similar photo as in Figure 2C was taken after 24 h, confirming that TCEP irreversibly reduces disulfide bonds.[69]

The influence of the temperature on the disulfide bond formation rate is shown in Figure 3 for 2 wt % of Na-alg-cys-900 in MOPS. At 37 °C, more than 50% of the initial thiol reacted after 2 days, while only a limited amount did so at 4 °C. After an almost linear decrease of the thiol concentration during the first two days, the reaction leveled off until day 6 probably due to reduced mobility of the polymer chains in the hydrogel. The viscosity of the solution strongly increased upon gelation by disulfide bond formation. This viscosity increase reduced the chain mobility and consequently hindered the thiol groups to approach and further react. The low conversion rate at 4 °C is advantageous for the solution preparation and storage of the solution prior to cell microencapsulation

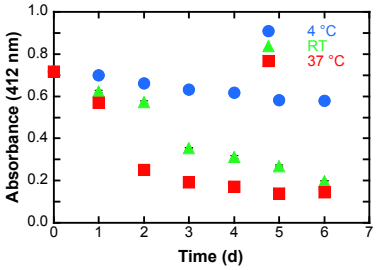

Figure 3. Gelation kinetics of Na-alg-cys-900 (2 wt % in MOPS) at different temperatures. The decrease of the absorbance at 412 nm refers to the thiol consumption.[57]

Combining the information presented in Figures 2 and 3, it is tempting to suggest that for a high degree of grafting, such as for Na-alg-cys-900, even a relatively low conversion of thiol groups after about 36 h at RT is sufficient to form a stable covalently crosslinked hydrogel.[68]

For another product, which was obtained by conjugating cystein hydrochloride to alginic acid, no spontaneous disulfid bond formation was reported. Instead, both the new thiol and carboxyl functionality added to the alginate backbone by this synthesis pathway participated in complexation with divalent zinc cations.[70]

Microsphere Formation. The slowly occurring covalent disulfide bond formation impairs the production of spherical hydrogels when this is done using simple extrusion technology. Neither of the two modified Na-alg types yielded stable MS without the support of ionic crosslinking. Both 1-comMS and 2-comMS were fabricated by extruding either Na-alg-PEG solutions alone or mixtures of Na-alg-cys/Na-alg solutions into the gelation bath containing $CaCl_2$ as ionic crosslinker. Simultaneously occurring ionic and covalent crosslinking was confirmed by exposing the MS either to sodium citrate, which interferes the ionic links, or to TCEP, which chemically reduces the covalent bonds.[69] This is demonstrated in Figure 4 for 2-comMS. While Ca-alg MS prepared from pure Na-alg solutions dissolved upon exposure to sodium citrate, the 2-comMS remained stable and maintained their spherical shape and size.

Different from Na-alg-PEG, Na-alg-cys alone did not form covalently reinforced 1-comMS at any degree of grafting. At very low degree of grafting, approx. 5% according to Ellman's assay, MS were formed but dissolved upon exposure to sodium citrate due to an insufficient number of covalent crosslinks. Increasing the degree of grafting above this value, Na-alg-cys droplets did not yield stable MS in the gelation bath, but either dissolved or formed irregularly shaped gels. This can be attributed to too slowly occurring ionic crosslinking probably due to the lack of sufficient residual carboxylic groups. Another factor causing badly shaped gels is chain degradation that occurred during the synthesis. Indeed, because of the relatively low viscosity of the Na-alg-cys-900 solutions, the droplets entered the gelation bath not at all, or only in deformed shape. Mixing Na-alg-cys with native Na-alg overcame this problem. The presence of Na-alg ensured fast gelation while maintaining the spherical shape of the droplet and Na-alg-cys reinforced the initially formed hydrogel by forming an interpenetrating covalently crosslinked gel structure.

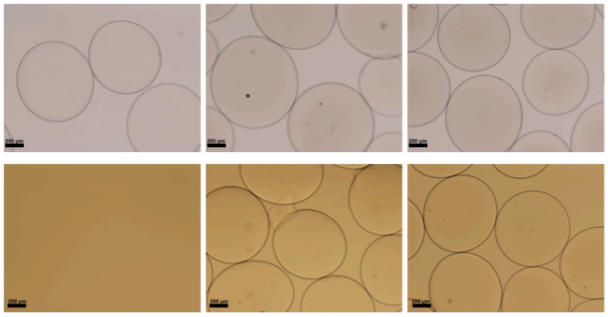

Figure 4. Stability of MS upon exposure to sodium citrate. Upper row (left to right): 3 wt % Na-alg alone; 2 wt % Na-alg + 1 wt % Na-alg-cys-900; 1 wt % Na-alg + 2 wt % Na-alg-cys-900; lower row: same batches after treatment with sodium citrate (100 mM) for 24 h; bars 200 µm.

The length of the grafted side chain presents an important difference between Na-alg-PEG and Na-alg-cys. While the short cysteamine graft (Scheme 2) certainly favors sterically the ionic crosslinking, it limits the probability of covalent links. The opposite situation applies for the Na-alg-PEG grafted in this study with a PEG derivative of 2000 g mol^{-1}, corresponding to a degree of polymerization of about 45 (Scheme 1). The flexibility of the longer side chain will certainly favor covalent links.

Microsphere Characterization. The major aim of this study was to demonstrate to which extent the functionalization of Na-alg could overcome some known shortcomings of the physical properties of Ca-alg MS, which are in particular their limited mechanical resistance, insufficient durability, and high permeability.[5,7,8,14-17] To this end, the MS were evaluated with respect to swelling behavior, size and chemical stability in different media, water uptake, mechanical resistance to compression, and permeability. The comparison of 1-comMS and 2-comMS was not the primary interest.

However, discussing improvements one has to be aware of the extreme variability of the natural compound Na-alg including the alternation of the guluronic and mannuronic units along the polymer backbone, the molar mass and the molar mass distribution. All these macromolecular peculiarities, and also the Na-alg concentration and the gelation technology, affect the hydrogel properties of the Ca-alg MS. These topics have been widely published and reviewed in the literature.[10,14,71,72]

Swelling/shrinking. Table 2 and Figure 5 show the swelling/shrinking behavior of 1-comMS when transferred from the gelation bath into water, at RT and 37 °C. The ionic strength in water is lower than in the gelation bath ($CaCl_2$, MOPS). As a consequence, an extension of the ionic polymer network is expected when MS are put in water. The data in Table 2 reflect this extension quantitatively and show the influence of the polymer concentration. A higher Na-alg-PEG concentration yielded denser croslinked hydrogels due to the potentially higher amount of ionic and covalent crosslinks per volume unit.

Table 2. Diameter of 1-comMS Prepared from Two Different Concentrations of Na-alg-PEG-13 after 3 Days Storage in the Gelation Bath (d_3) and Subsequently Incubated for 48 h in Water at RT ($d_{48,\,water}$)

c[a] (wt %)	d_3 (µm)	$d_{48,\,water}$ (µm)	Δd/ΔV (%)
2.5	557 ± 66	582 ± 75	+4.4 / +14
5.0	627 ± 70	639 ± 93	+2.0 / +6.0

[a]Concentration of the polymer in MOPS (10 mM, pH=7.4)

Storage at 37 °C for one month confirmed the hydrogel stability over this period (Figure 5). To ensure complete covalent crosslinking, the MS were first kept for 6 days in the gelation bath before transferring them in water. After initial expansion in water, no further significant size variation was observed over 4 weeks at 37 °C. In view of future biomedical application, the MS integrity and stability was evaluated in several culture media and was confirmed not only for MOPS but also for DMEM and RPMI over a period of two months at 37 °C.

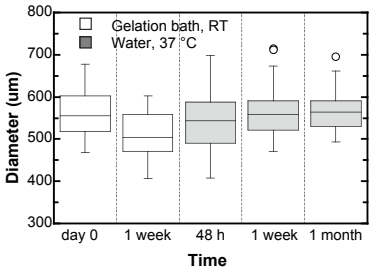

Figure 5. Influence of the medium and temperature on the 1-comMS size (3.5 wt %) at RT in the gelation bath and at 37 °C in water (box plot, n=30).

Four formulations (Table 3) have been used to estimate the physical properties of the 2-comMS. Pure Ca-alg MS were prepared at the same total concentrations indicated in Table 3 and used for comparison.

Upon exposure of the 2-comMS of formulations 1-4 and appropriate Ca-alg MS to aqueous sodium citrate solutions (5 mM), differences in terms of water uptake capacity related to 1 g polymer became obvious (Figure 6A). Such a low citrate concentration only slightly weakens the ionic network but ensures the integrity of the MS. Comparing the total initial polymer concentrations in Table 3 with the polymer concentrations calculated from the data shown in Figure 6A, a dilution/volume swelling by a factor of 2.0-2.2 was evident for Ca-alg MS while for the 2-comMS shrinking by a factor of 0.8-0.7 was observed. However, it cannot be excluded that the droplet shrinking took already place during the covalent crosslinking, before the MS were transferred into the citrate solution. Taking formulation 3 as example, the initial polymer concentration of 2.5 wt % reduced to 1.16 wt % in the Ca-alg MS but increased to 3.51 wt % in the 2-comMS (Figure 6B). This clearly demonstrates the reinforcement of the hydrogel by Na-alg-cys. At this low sodium citrate concentration, the Ca-alg MS remained intact but strongly swelled. Assuming a similar weakening of the ionic network in the 2-comMS suggests that the network properties are governed by the covalent crosslinks. Even for formulation 1, where only 0.5 wt % of Na-alg-cys was present, the concentration increased from 1.5 wt % to 1.9 wt %, but decreased to from 1.5 wt % to 0.7 wt % for the pure Ca-alg (Figure 6B).

Table 3. Composition of 2-comMS Preparations in MOPS (10 mM, pH=7.4)

formulation	total (wt %)	Na-alg-cys-900 (wt %)	Na-alg[a] (wt %)
1	1.5	0.5	1.0
2	2.0	1.0	1.0
3	2.5	1.5	1.0
4	3.0	2.0	1.0

[a] Kelton LV

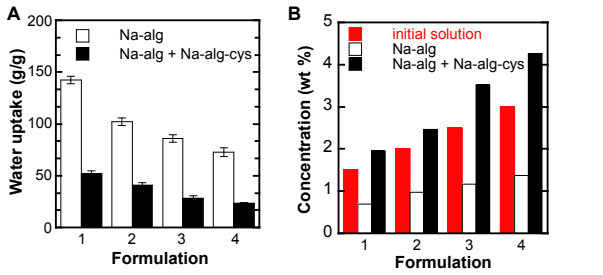

Figure 6. Influence of the MS composition on water uptake and final polymer concentration in the MS. (A) 2-comMS formulations and MS prepared from pure Na-alg, 48 h exposure to 5 mM sodium citrate at RT (average ± SD, n=3); (B) polymer concentration after 48 h, calculated from average values in (A).

Mechanical properties. The measurement of the mechanical resistance to uniaxial compression three days after the formation of 1-comMS ensured the completion of disulfide bond formations. Typical compression curves are presented in the SI (SI 6, Figure S5).

Minimal mechanical resistance was monitored when compressing the MS until 40-50% of their initial diameter, followed by a slight increase until around 70%, before becoming exponential until 90% compression. Figure 7A presents the mechanical resistance at 90% compression of 1-comMS prepared in the concentration limits 2.5 to 5.0 wt % where MS can be formed. The resistance increased with the Na-alg-PEG concentration but remained in the range of pure Ca-alg MS. Nevertheless, improvement of the mechanical properties was achieved in terms of shape recovery upon repeated compression to 90% of the MS diameter (Figure 7C). The known heterogeneous gelation of Na-alg, in particular at higher Na-alg concentration, is one possible reason for this phenomenon.[55] With

increasing Na-alg concentration, a maximum of recovery performance was passed: MS of 2.5 wt % Na-alg performed better than MS of 4 wt % Na-alg. The improvement for the 1-comMS is attributed to covalent crosslinking. Figures 7B and 7D present the comparison of the mechanical properties for 2-comMS and Ca-alg. The better mechanical resistance to one and multiple compressions is evident, and ascribed to the covalent crosslinking of the cysteamine grafted Na-alg inside the Ca-alg matrix. Moreover it is likely that the Na-alg-cys also participates in the ionic crosslinking by calcium ions.

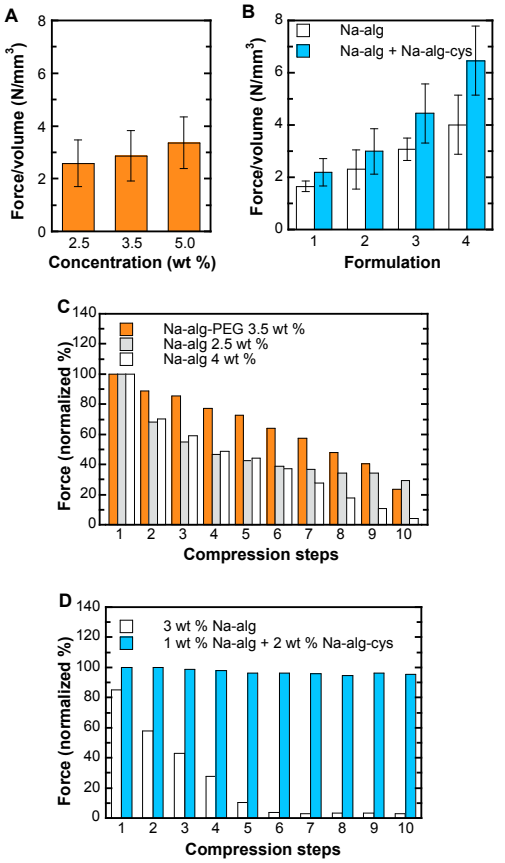

Figure 7. Mechanical resistance to uniaxial compression to 90 % of the initial MS diameter. (A) increase of the mechanical resistance of 1-comMS with the Na-alg-PEG-13 concentration; (B) increase of the resistance as a function of the composition of 2-comMS and Ca-alg MS; (C) resistance to 10 successive compressions of 1-comMS (3.5 wt %) and Ca-alg (2.5 and 4 wt %); (D) resistance to 10 successive compressions of 2-comMS (formulation 4 in Table 3) and Ca-alg MS.

Permeability. 150 kg mol^{-1} is generally considered a threshold above which MS intended for cell microencapsulation and subsequent transplantation should exclude any compound. This threshold can hardly be achieved by Ca-alg. The results of the permeability assessment by ingress diffusion of FITC-Dextran standards are shown in Figure 8 and in SI 7 Figure S6. While FITC-Dextran of 40 kg mol^{-1} permeated all MS types formed at any composition and polymer concentration, MS produced using Na-alg-PEG-13 at 5 wt % completely exclude FITC-Dextran 70 kg mol^{-1} (Figure 8B). Consequently, the MWCO can be expected between 40 and 70 kg mol^{-1}. Such a dense polymer network could be achieved neither for Na-alg-PEG-11 nor for the 2-comMS or Ca-alg, even not at the highest concentrations tested in terms of mechanical stability. A minimum of 2 wt % Na-alg-cys-900 is needed in the 2-comMS formulation to ensure a MWCO of 150 kg mol^{-1} (SI 7, Figure S6). Worth mentioning, the permeability is not a static value but depends strongly on the environment of the MS.[71]

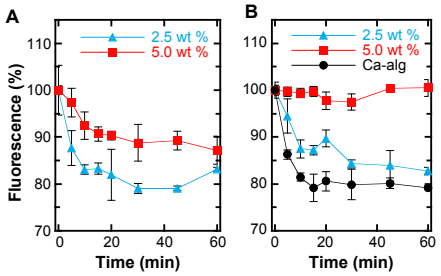

Figure 8. Influence of the Na-alg-PEG-13 concentration on the permeability of 1-comMS, assessed by ingress diffusion of FITC-Dextran, (A) 40 kg mol^{-1}, (B) 70 kg mol^{-1}, (average ± SD, n=3).

Cell Microencapsulation. The feasibility of cell microencapsulation in 1-comMS and 2-comMS (diameter 500-600 µm) was confirmed using primary human foreskin fibroblasts as model cells.[54] The cells were homogeneously distributed within both MS types (Figures 9A, 9D).

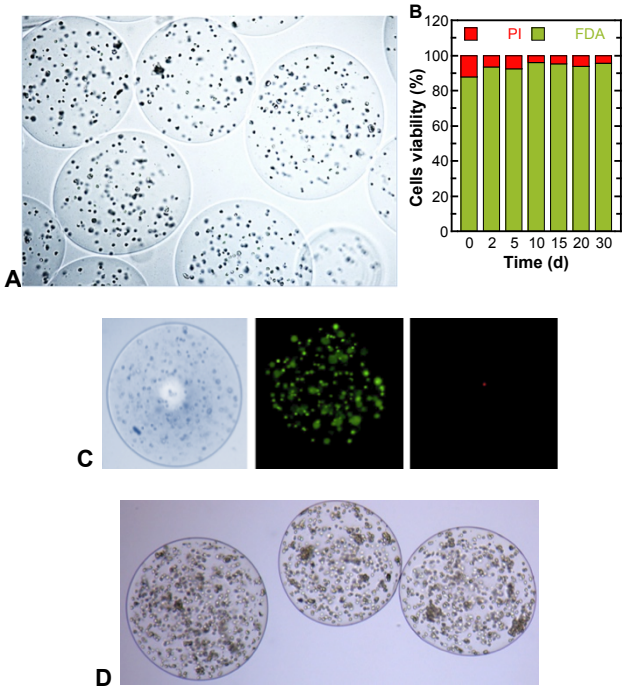

Figure 9. Microencapsulation of EDX cells. (A) at day 0 in 1-comMS, Na-alg-PEG-13 3.5 wt %; (B) viability of microencapsulated EDX cells; (C) at day 30, from left to right: light microscopy, viability staining of the same object with FDA (green: living cells), PI staining (red: dead cells); (D) at day 0 in 2-comMS, 2 wt % Na-alg-cys + 1.5 wt % Na-alg.

Furthermore, no free EDX cells were identified in the gelation bath indicating no out-diffusion of the cells from the polymer solution drops during the gelation process. Thus, the fact that covalent crosslinking immediately after the extrusion into the gelation bath is incomplete seemed not to be unfavorable. The cell viability assessed by FDA/PI staining, revealed good survival immediately after the microencapsulation process and during a subsequent 4-week culture (Figures 9B, 9C). No significant decrease in cell viability compared to free cells was observed suggesting that the new PEG-modified and cys-modified Na-alg are cytocompatible.

CONCLUSIONS

Two synthesis principles were presented which add tailor-made thiol chemical self-crosslinking functionality to the biopolymer sodium alginate either as thiol end groups of grafted heterobifunctional PEG or as cysteamine. It was proven that ionic gelation with calcium ions and covalent self-crosslinking of the thiol groups occurred simultaneously and lead to the targeted improvement of the mechanical properties and permeability compared to pure Ca-alg MS. The degree of grafting, polymer concentration, and chemical composition were identified as the critical parameters to vary the MS properties and adapt these to future cell microencapsulation applications. Preliminary in vitro studies demonstrated cytocompatibility of the materials and process, but this has to be confirmed for other cell types and specific applications.

In particular favorable are the absence of both polycations and chemical crosslinkers as well as the mild and simple one-step MS formation process, which can take place in cell culture media. The availability of such novel hydrogel materials that can be manufactured as microspheres with adaptable properties suitable for cell microencapsulation is considered crucial for accelerating the progress and clinical translation of innovative cell therapies.

Moreover, from the gelation mechanisms of the formulations containing the novel synthesized alginate derivatives, suitability for other technologies including microfluidics can be concluded. Finally, the selected synthesis pathways and functional end groups added to the alginate backbone offer the possibility to conjugate bioactive compounds for controlled and localized release in specific applications. Overall, the two novel MS types extend the materials basis for cell microencapsulation.

AUTHOR INFORMATION

Corresponding Authors

* Christine.wandrey@epfl.ch (C.W.); Tel.: +41-21-693-9661; Fax: +41-21-693-9685.

* Sandrine.gerber@epfl.ch (S.G.-L.); Tel.: +41-21-693-9372; Fax: +41-21-693-5550

Present Addresses

‡ R.M., University of Toronto, Institute for Biomaterials and Biomedical Engineering, CCBR, 160 College Street, M5S 3E1, Toronto ON, Canada

Author Contributions

The manuscript was written through contributions of all authors. All authors have given approval to the final version of the manuscript.

‡ R.M., F.B. and V.C. contributed equally;

S.G.-L., L.B., and C.W. directed the project.

Funding Sources

Swiss National Science Foundation (SNSF grants 205321_141286/1 and CR 23I2_152974/1) Commission for Technology and Innovation (CTI grant 13804.1 PFLS-LS), Foundation InsuLeman, Geneva.

Notes

The authors declare no competing financial interest.

ASSOCIATED CONTENT

Supporting Information. Synthesis protocols; Solution preparation protocols; ^{1}H-NMR and ^{13}C-NMR spectra; Microsphere characterization. This material is available free of charge via the Internet at http://pubs.acs.org.

ACKNOWLEDGMENT

The authors acknowledge financial support from the SNSF (grants 205321_141286/1 and CR 23I2_152974/1), the CTI (grant 13804.1 PFLS-LS) and the Foundation InsuLeman, and thank H.-J. Schuurman for critical revision of the manuscript.

ABBREVIATIONS

DMSO, dimethyl sulfoxide; EDC, N-(3-dimethylaminopropyl)-N′-ethylcarbodiimide hydrochloride; EDX, primary human foreskin fibroblasts; FDA, fluorescein diacetate; FITC, fluorescein isothiocyanate; HV, high viscous; LV, low viscous; MES, 2-(N-morpholino) ethanesulfonic acid; MOPS, 3-(N-morpholino)propanesulfonic acid; MWCO, molecular weight cut-off; Na-alg, sodium alginate; NHS, N-hydroxysuccinimide; PBS, phosphate buffered saline; PEG, poly(ethylene glycol); PI, propidium iodide; RT, room temperature; TBA, tetrabutylammonium substituent; TBAOH, tetrabutylammonium hydroxide; TCEP, tris(2-carboxyethyl)phosphine.

REFERENCES

(1) Lee, K. Y. ; Mooney, D. J. *Prog. Poly. Sci.* **2012**, *37*, 106-126.

(2) Goh, C. H.; Heng, P. W. S.; Chan, L. W. *Carbohyd. Polym.* **2012**, *88*, 1-12.

(3) Dimitriu, S. *Polymeric Biomaterials*, 2nd Ed, Marcel Decker Inc: New York, Basel 2002, 1-61

(4) Smidsrød, O.; Skjåk -Bræk, G. *Trends Biotechnol.* **1990**, *8*, 71-78.

(5) Mørch, Y. A.; Donati, I.; Strand, B. L.; Skjåk-Bræk, G. *Biomacromolecules* **2006**, *7*, 1471-1480.

(6) Draget, K. I.; Skjåk -Bræk, G.; Smidsrød, O. *Int. J. Biol. Macromol.* **1997**, *21*, 47-55.

(7) Nedovic, V.; Willaert, R. *Fundamentals of Cell Immobilization Biotechnology*; Kluwer Academic Publishers: Dordrecht, Boston, London, 2004.

(8) Nedovic, V.; Willaert, R. *Applications of Cell Immobilization Biotechnology*; Springer: Dordrecht, 2005.

(9) Figaro, S.; Pereira, U.; Dumé, A.-S.; Rada, H.; Capone, S.; Bengrine, A.; Baze, A.; Rabenirina, E.; Semenzato, N.; Herpe, Y.-E.; Faivre, J.; Dufresne, M.; Richert, L.; Duverlie, G.; Daujat-Chavanieu, M.; Saliba, F.; Pouchoulin, D.; Legallais, *IRBM*, **2015**, http://dx.doi.org/10.1016/j.irbm.2015.01.010.

(10) Lacik, I. *Micro Nanosyst.*, **2015**, *5*, 168-176.

(11) Meier R. P. H.; Mahou, R.; Morel, P.; Meyer, J.; Montanari, E.; Müller, Y. D.; Christofilopoulos, P.; Wandrey, C.; Gonelle-Gispert, C.; Bühler, L. H. *J. Hepatol.* **2014**, *62*, 634-641.

(12) Heng, B. C.; Aubel, D.; Fussenegger, M. *Curr. Opin. Biotech.* **2015**, *35*, 37-45.

(13) Folcher, M.; Oesterle, S.; Zwicky, K.; Thekkottil, T.; Heymoz, J.; Hohmann, M.; Christen, M.; El-Baba, M. D.; Buchmann, P.; Fussenegger, M. *Nat. Commun.* **2014**, *5:5392*, 1-11, doi:10.1038/ncomms6392.

(14) O'Sullivan, E. S.; Vegas, A.; Anderson D. G.; Weir, G. C. *Endocr. Rev.* **2011**, *32*, 827-844.

(15) Basta G.; Calafiore R. *Curr. Diab. Rep.* **2011**, *11*, 384-391.

(16) Drury, J. L.; Dennis, R. G:; Mooney, D. J. *Biomaterials* **2004**, *25*, 3187-3199.

(17) Moya, M. L.; Morley, M.; Khanna, O.; Opara, E. C.; Brey, E. M. *J. Mater. Sci.: Mater. Med.* **2012**, *23*, 903-912.

(18) Santos, E.; Orive, G.; Calvo, A.; Catena, R.; Fernandez-Robredo, P.; Garcia Layana, A.; Hernandez, R. M.; Pedraz, J. L. *J. Control. Release* **2012**; *158*, 443-450.

(19) Clayton, H. A.; London, N. J. M.; Colloby, P. S.; Bell P. R. F.; James, R. F. L. *J. Microencapsulation* **1991**, *8*, 221-233.

(20) Robitaille, R.; Pariseau, J. F.; Leblond, F. A.; Lamoureux, M.; Lepage, Y.; Halle, J. P. *J. Biomed. Mater. Res. Part A* **1999**, *44*, 116-120.

(21) King, A.; Strand. B.; Rokstad, A. M; Kulseng, B.; Andersson, A.; Skjåk-Bræk, G.; Sandler, S. *J. Biomed. Mater. Res. Part A* **2003**, *64*, 533-539.

(22) Juste, S.; Lessard, M.; Henley, N.; Ménard, M.; Hallé, J.-P. *J. Biomed. Mater. Res. Part A* **2005**, 389-398.

(23) Orive, G.; Tam, S. K.; Pedraz, J. L.; Hallé, J.-P. *Biomaterials* **2006**, *27*, 3691-3700.

(24) Darrabie, M. D.; Kendall, W. F.; Opara, E. C. *Biomaterials* **2005**, *26*, 6846-6852.

(25) Chen, A. Z.; Bai, Y.; Wang, S. B.; Liu, Y. G.; Chen, Z. X. *J. Biomimetics Biomater. Tissue Eng.* **2012**, 14, 53-64.

(26) Renken, A.; Hunkeler, D. *J. Microencapsulation* **2007**, *24*, 20-39.

(27) Wandrey, C.; Espinosa, D.; Rehor, A.: Hunkeler, D. *J. Microencapsulation* **2003**, *20*, 597-611.

(28) Zhang, L. Y.; Yao, S. J.; Guan, Y. X. *Process Biochem.* **2005**, *40*, 189-193.

(29) Zhao, W.; Zhang, Y.; Liu, Y.; Tan, M.; Yu, W.; Xie, H.; Ma, Y.; Sun, G.; Lv, G.; Zhao, S.; Ma, X. *J. Chem. Technol. Biotechnol.* **2012**, *88*, 449-455.

(30) Baruch, L.; Machluf, M. *Biopolymers* **2006**, *82*, 570-579.

(31) Chen, F.; Tian, M.; Zhang, D.; Wang, J.; Wang, Q.; Yu, X.; Zhang, X.; Wan, C. *Mater. Sci. Eng. C* **2012**, *32*, 310-320.

(32) Xu, K.; Fu, Y.; Chung, W. *Acta Biomater.* **2012**, *8*, 2504-2516.

(33) Fu, Y.; Xu, K.; Zheng, X.; Giacomin, A. J.; Mix, A. W.; Kao, W. J. *Biomaterials* **2012**, *33*, 48-58.

(34) Phelps, E. A.; Enemchukwu, N. O.; Fiore, V. F.; Sy, J. C.; Murthy, N.; Sulchek, T. A.; Barker, T.H.; Garcia, A. J. *Adv. Mater.* **2012**, *24*, 64-70.

(35) Mazumder, M. A. J.; Shen, F.; Burke, N. A. D.; Potter, M. A.; Stöver H. D. H. *Biomacromolecules*, **2008**, *9*, 2292-2300.

(36) Silva, C. M.; Ribeiro, A. J.; Ferreira, D.; Veiga, F. *Euro. J. Pharm. Sci.* **2006**, *29*, 148-159.

(37) Rokstad, A. M.; Brekke, O. L.; Steinkjer, B. Ryan, L.; Kolláriková, G.; Strand, B. L.; Skjåk-Bræk, G.; Lacík, I.; Espevik, T.; Mollnes, T. E. *Acta Biomater.* **2011**, *7*, 2566-2578.

(38) Strand, B. L.; Ryan, T. L.; Kulseng, B.; Ryan, L.; Kolláriková, G.; Strand, B. L.; Skjåk-Bræk, G.; Lacík, I.; Espevik, T.; Mollnes, T. E. *Cell Transplant* **2001**, *10*, 263-275.

(39) Rokstad, A. M.; Brekke, O. L.; Steinkjer, B.; Ryan, L.; Kolláriková, G.; Strand, B. L.; Skjåk-Bræk, G.; Lacík, I.; Espevik, T.; Mollnes, T. E. *Biomaterials* **2013**, *34*, 621-630.

(40) Tam, S. K.; Bilodeau, S.; Dusseault, J. Langlois, G.; Halle, J. -P.; Yahia, L. H. *Acta Biomater.* **2011**, *7*, 1683-1692.

(41) Gattás-Asfura, K.; Fraker, C. A.; Stabler, C. L. *J. Biomed. Mater. Res. Part A* **2012**, *100A*, 1963-1971.

(42) Pawar, S. N. ; Edgar, K. J. *Biomaterials* **2012**, *33*, 3279-3305.

(43) Wu, M.; Ni, C.; Yao, B.; Zhu, C.; Huang, B.; Zhang, L. *Polym. Eng. Sci.* **2013**, *53*, 1583-1589.

(44) Dolgin, E. *Nat. Med.* **2014**, *20*, 9-11.

(45) Roshanbinfar, K.; Salahshour Kordestani, S. *J. Biomater. Tissue Eng.* **2013**, *3*, 185-189.

(46) Sawhney, A. S.; Hubbell, J. A. *Biomaterials* **1992**, *13*, 863-870.

(47) Gattás-Asfura, K.; Stabler, C. L. *Biomacromolecules* **2009**, *10*, 3122-3129..

(48) Hall, K. K.; Gattás-Asfura, K.; Stabler, C. L. *Acta Biomater.* **2011**, *7*, 614-624.

(49) Tomei, A. A.; Manzoli, V.; Fraker, C. A.; Giralod, J.; Velluto, D.; Najjar, M.; Pileggi, A.; Molano, R. D.; Ricordi, C.; Stabler, C. L., Hubbell, J. A. *PNAS*, **2014**, *111*, 10514-10519.

(50) Miao, T.; Rao, K. S.; Spees, J. L.; Oldinski, R. A. *J. Control. Release* **2014**, *192*, 57-66.

(51) Zhang, Z.; Loebus, A.; de Vicente, G.; Ren, F.; Arafeh, M.; Ouyang, Z.; Lensen, M. C. *Chem. Mater.* **2014**, *26(12)*, 3624-3630.

(52) Mahou, R.; Tran, N. M.; Dufresne, M.; Legallais, C.; Wandrey, C. *J. Mater. Sci.: Mater. Med.* **2011**, *23*, 171-179.

(53) Mahou, R.; Wandrey, C. *Macromolecules*, **2010**, *43*, 1371-1378.

(54) Mahou, R.; Meier, R. P. H.; Bühler, L. H.; Wandrey C. *Materials* **2014**, *7*, 275-286.

(55) Sainz Vidal-Serp, D. **2004**, PhD-Thesis 3052, EPFL, Lausanne Switzerland.

(56) Mahou, R. **2011**, PhD-Thesis 5163, EPFL, Lausanne, Switzerland.

(57) Ellman, G. *Arch. Biochem. Biophys.* **1958**, *74*, 443-450.

(58) Winther, J. R.; Thorpe, C. *Biochim. Biophys. Acta*, **2014**, *1840*, 838-846.

(59) Gomez, C. G.; Rinaudo, M.; Villar, M. A. *Carbohyd. Polym.* **2007**, *67*, 296-304.

(60) Carré, M.-C. ; Delestre, C. ; Hubert, P. ; Dellacherie, E. *Carbohydr. Polym.* **1991**, *16*, 367-379.

(61) Cathell, M. D. ; Szewczyk, J. C. ; Schauer, C. L. *Mini-Rev. Org. Chem.* **2010**, *7*, 61-67.

(62) Pawar, S. N. ; Edgar K. J. *Biomacromolecules* **2011**,*12*, 4095-4103.

(63) Pawar, S. N.; Edgar, K. J. *Biomaterials* **2012**, *33*, 3279-3305.

(64) Le-Tien, C. ; Millette, M. ; Mateescu, M.-A. ; Lacroix, M. *Biotechnol. Appl. Biochem.* **2004**, *39*, 347-354.

(65) Eiselt, P.; Lee, K. Y.; Mooney, D. J. *Macromolecules* **1999**, *32*, 5561-5566.

(66) Yang, J.-S.; Xie, Y.-J.; He, W. *Carbohyd. Polym.* **2011**, *84*, 33-39.

(67) Gilles, M. A.; Hudson, A. Q.; Borders, C. L. *Anal. Biochem.* **1990**, *184*, 244-248.

(68) Witt, D. *Synthesis*, **2008**, *16*, 2491-2509.

(69) Burns, J. A.; Butler, J. C.; Moran, J.; Whitesides, G. M. *J. Org. Chem.* **1991**, *56*, 2648-2650.

(70) Taha, M. O.; Aiedeh, K. M.; Al-Hiari, Y.; Al-Khatib, H. *Pharmazie* **2005,** *60*, 736–742.

(71) de Vos, P.; Bucko, M.; Gemeiner, P.; Navratil, M.; Svitel, J.; Faas, M.; Strand, B. L.; Skjåk -Bræk, G.; Mørch, Y. A.; Vikartovska, A.; Lacik, I.; Kollarikova, G.; Orive, G.; Poncelet, D.; Pedraz, J. L.; Ansorge-Schumacher, M. B. *Biomaterials* **2009**, *30*, 2559-2570.

(72) Mercadé-Prieto, R.; Zhang, Z. *J. Microencapsulation* **2012**, *29*, 277-285.

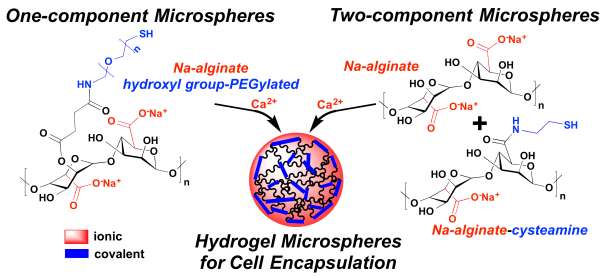
One-component Microspheres
Two-component Microspheres
Na-alginate
hydroxyl group-PEGylated
Na-alginate
Ca2+
Ca2+
ionic
covalent
Hydrogel Microspheres
for Cell Encapsulation
Na-alginate-cysteamine